

An Innovative Beneficial Reclamation of Flue Gas Desulfurization Brine Using Bipolar Membrane Electrodialysis Technique

Min Xia, Chunsong Ye*, Rong Cao, Haoyu Huang, Jianwei Huang

School of Power and Mechanical Engineering, Wuhan University, Wuhan 430072, Hubei, China

*E-mail: chunsongye@126.com

Received: 9 August 2017 / Accepted: 21 March 2018 / Published: 10 May 2018

Flue gas desulfurization (FGD) brine containing high salinity poses a significant challenge to the implementation of environmental policy in china. In this work, an innovative alternative approach of bipolar membrane electrodialysis (BMED) technique has been proposed to effectively reuse this brine by the acid and base production on the premise of zero emission requirements. The experimental results demonstrate that the high acid and base concentrations in excess of 1.0 mol/L can be obtained with the satisfactory desalination. Higher initial salt concentration shows nearly no significant change on current efficiency, acid/base concentration and acid volume. Nevertheless, appropriate concentration for $\times 2$ of FGD brine is necessary and beneficial for acid/base production by the decrease of energy consumption from 2.34 to 2.14 Kwh/kgNaOH. Additionally, the ions migration between Cl^- and SO_4^{2-} indicates high purity HCl with little H_2SO_4 contamination can be obtained if the initial salt concentration of FGD brine is improved in the earlier acid production. In conclusion, BMED presents a high potential for FGD brine treatment in view of environmentally friendly as well as attractive economic benefit.

Keywords: flue gas desulfurization brine; bipolar membrane electrodialysis; acid/base production; desalination

1. INTRODUCTION

Recently, environmental concerns for natural waters contamination by industrial brine are more highly focused in industrialized nations [1]. With the issue of stricter environmental regulations, guidelines and policies, especially the zero emission requirement (*i.e.* that no liquid may be discharged to the environment) in China [2], effluent reclamation and reuse have received more and more attention. Appropriate management of the stream is necessary and is identified as an opportunity to

develop circular concepts to convert the waste into a resource for materials production. For example, the reverse osmosis (RO) brine abundant in sodium chloride has been reported to reuse in chlorine alkali industry as the production of chlorine and sodium hydroxide [3].

In thermal power plants, the hypersaline brine comes from the flue gas desulfurization (FGD) process employing limestone-gypsum method [4] after the hydrocyclone separation of gypsum. The brine has complex composition with high total dissolved solids (TDS) [5] containing primary elements of Ca, Mg, S, Cl. Its composition distributions are strong depending on the type of coal burned and limestone slurry cycled in desulfurizer [6].

The zero emission requirements for FGD brine disposal were mainly terminated by thermal evaporation technique [7] with the purpose of crystallization for solid salt and fresh water recovery. Although thermal treatment is technical available, it presents several limitations regarding economic feasibility such as unacceptable investment and operation costs [8]. For that reason, electrically driven membrane separation process using electrodialysis in combination of bipolar membranes (BMED) would be a promising technology in terms of not only brine minimization but also increase of reusability and recyclability of waste through chemical production alternative [9-10]. Once the reverse voltage is imposed between the electrodes of BMED stack, the polarization process of the bipolar membrane (BPM) will take place rapidly to split the water molecules into H^+ and OH^- and this water dissociation process is accelerated up to 50 million times compared to the rate in aqueous solution. Therefore, the produced H^+ and OH^- ions can be used to generate corresponding acid (HX) and base (MOH) from salts (MX) [11] with the perfect separation by ion exchange membrane (*i.e.* anion across the anion exchange membrane (AEM) impeded by the cation exchange membrane (CEM), cation across CEM hindered by AEM). In comparison with traditional electrolytic electrodialysis (EED) process for acid/base production through electrode reaction, the theoretical energy consumption for BPM is much lower than that for electrode reaction. Furthermore, the BMED stack structure is more compact with the high repeating unit number rather than only one from EED stack, which is beneficial to improve acid/base productivity.

Currently, the BMED has various potential applications, mainly situated in chemical process industry as well as in biotechnology [12]. In industrial brine treatment aspect, much applications of BMED concentrate on RO brine reclamation [10-11, 13-15]. Ibáñez et al [14] applied the BMED to produce the acid and base from RO brine and demonstrated it was technically feasible for the production of 1.0 mol/L or higher concentrated acid/base with the current efficiency above 60%. Reig et al [11] discussed the influence of initial salt and acid/base concentration to the energy consumption and acid/base concentration. And further study has also been investigated [15] through integration of nanofiltration for hardness removal and BMED for acid/base production. Approximately 1 mol/L NaOH/HCl could be obtained using the constant voltage of 9 V with the energy consumption 2.66 Kwh/kgNaOH and current efficiency 77%. Other industrial brines such as glyphosate neutralization liquor, spent caustic and textile wastewater [16-18] have also been reported using BMED for acid/base production. However, regarding the FGD brine with high salt concentration, few works have been involved in technical and economic feasibility so far.

In a perfect BMED process, water transport and co-ion leakage could be neglected with the salt ions completely shifting into corresponding acid and base compartment, which means so long as the

initial salt content in the salt compartment (the product of salt concentration and salt volume) and initial acid/base volume in the acid/base compartment are fixed, we can deservedly infer the final acid and base concentration in the solutions. In fact water transport and co-ion leakage always seriously affect the acid/base production efficiency and the degree of desalination. In this work, the investigation focused specifically on simulated brine from power plant FGD process for resourceful utilization. The concentration times for simulated FGD brine was primarily evaluated with respect to the influence of acid/base production, co-ion leakage, acid/base volume, anion migration, current efficiency and energy consumption through maintaining the constant salt content.

2. EXPERIMENTAL

2.1. Materials and chemicals

Table 1. Chemical compositions of original and synthetic FGD brine.

Parameters	Units	Composition of FGD brine	
		Synthetic	Original
pH	/	6.8	7.30
Conductivity	ms/cm	42.8	30.3
Cations			
Na ⁺		11730(510)	1180 (51.3)
NH ₃ -N	mg/L (mM/L)	/	77.6 (5.5)
Ca ²⁺		/	790 (19.8)
Mg ²⁺		/	4752 (198)
Anions			
Cl ⁻		9572 (270)	9601 (270.8)
SO ₄ ²⁻	mg/L (mM/L)	11520 (120)	11080 (115.4)
NO ₃ ⁻		/	105.5 (1.7)

Table 2. The characteristics of membranes used for BMED stack.

Items	Membranes		
	CJMC-1 (CEM)	CJMA-1 (AEM)	CJBPM-1 (BPM)
Type	Homogeneous	Homogeneous	Homogeneous
Thickness(μm)	140-150	90-100	150-180
Water uptake (% dry)	35-40	15-20	45-55
IEC (meq/g)	0.8-1.0	0.8-1.0	/
Electric resistance (Ω·cm ²)	1.5-2.5	2.5-3.5	/
Transference number (%)	>98	>94	/

FGD brine was supplied by a power plant located in Guangdong province, China. Its chemical compositions were summarized in Table 1. Considering Mg and Ca were predominance over cation ions, these ions therefore should be removed first prior to BMED operation in order to avoid membrane fouling and scaling [19]. For practical purposes and taking into account that the Ca and Mg purification process was evaluated previously, the eliminated hardness ions could be replacement of sodium [20]. Hence, the mixture of NaCl and Na₂SO₄ brines (shown in Table 1) simulating the composition of original FGD brine to be used in the valorization as HCl, H₂SO₄ and NaOH by BMED was prepared in the present work. The membranes used for the experiments were purchased from Kejia Polymer Materials Co., Ltd, Hefei, China. And their characteristics were tabulated in Table 2. Other reagents were all of analytical grade manufactured by Sinopharm Chemical Reagent Co., Ltd, Shanghai, China.

2.2. Experimental description on BMED setup

Table 3. Experimental conditions for BMED running.

Run	Salt concentration ^a	Salt content	Current density	Acid (base)	electrode rinse	Flow velocity
Batch 1	×1	0.918 mol Na ⁺ 0.486 mol Cl ⁻ 0.216 mol SO ₄ ²⁻	30 mA/cm ²	600 mL	600 mL 0.3mol/L Na ₂ SO ₄	30 L/h
Batch 2	×1.2					
Batch 3	×1.5					
Batch 4	×2					
Batch 5	×3					

^a represents the salt concentration relative to synthetic FGD brine.

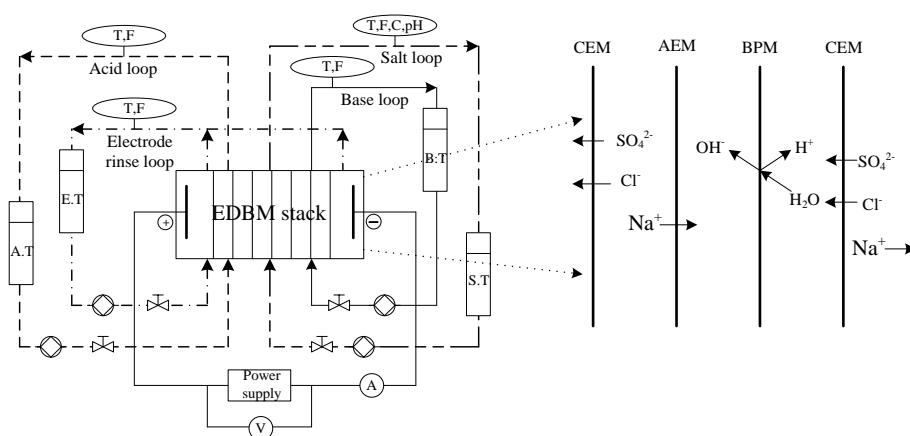


Figure 1. Scheme diagram of the BMED setup and one cell trio configuration (T: temperature sensor, F: flowmeter, pH: pH meter, C: conductivity sensor, A: ammeter, V: voltmeter, S.T: salt tank, A.T: acid tank, B.T: base tank, E.T: electrode rinse tank, CEM: cation exchange membrane, AEM, anion exchange membrane, BPM: bipolar membrane).

Scheme diagram of the BMED setup with the closed loop model is presented in Fig 1. The setup provided by Kejia Polymer Materials Co., Ltd, Hefei, China was composed of 16 pieces of membranes in total alternated with CEM, AEM, BPM and CEM as one cell trio configuration. Both of CEM ends were terminated by two electrodes made of titanium coated with ruthenium. The effective area of each membrane was 189 cm^2 with the dimension of $21 \text{ cm} \times 9 \text{ cm}$. The compartments for electrode rinse, acid, base and salt solution were separated by silicone partition net pacers with thickness of 0.80 mm , and connected to four diaphragm pumps ($0\text{-}50 \text{ L/h}$) to provide circulating power of feed solution. A regulated CV/CC power supply with the specification of maximum permissible voltage 60 V input and current 10 A output was applied to drive water dissociation. The specific experiment conditions in this work were given in Table 3 with the constant salt content by changing the initial salt concentration. Ideally, the concentration of both acidity and basicity would reach 1.53 mol/L . Prior to applying electric field for the BMED stack, each compartment should be cycled enough time to eliminate visible bubbles existing in feed solution [21]. All the experiments were carried out in the batch mode, upon the conductivity in the salt compartment decreased to 5 ms/cm , the experiment was immediately interrupted as one batch.

2.3. Data analysis

In order to efficiently evaluate the economic feasibility of BMED for FGD brine reclamation, current efficiency and energy consumption for acid/base production should be investigated in this work. The current efficiency (η) means the proportion of theoretical charges that required for H^+ or OH^- formation to the practical consumption, value of which is calculated by the following equation.

$$\eta(\%) = \frac{zF(C_t V_t - C_0 V_0)}{NIt} \times 100 \quad (1)$$

The energy consumption for yielded sodium hydroxide (E , kWh/kg) is calculated using the integral formula, expressed in Eq. (2)

$$E = \int_0^t \frac{UIt}{C_t V_t M_b} \quad (2)$$

where C_0 and C_t are the concentration of OH^- in the base compartment at time 0 and t (mol/L), respectively, z is the absolute valence, V_t is the circulated base volume at time t (L), F is the Faraday constant ($96,500 \text{ C mol}^{-1}$), I is the current (A), N is the repeating unit numbers, U is the voltage drop across the BMED stack (V) and M_b is the molecular weight of NaOH (40 g/mol).

Additionally, anion exchange membrane selectivity for chlorine and sulfate is also discussed in this work according to the method introduced by Van der Bruggen et al[22]. The separation efficiency between chlorine and sulfate could be obtained as follows

$$S_{Cl^-}^{SO_4^{2-}}(t) = \frac{(c_{SO_4^{2-}}(t)/c_{SO_4^{2-}}(o)) - (c_{Cl^-}(t)/c_{Cl^-}(o))}{(1 - c_{SO_4^{2-}}(t)/c_{SO_4^{2-}}(o)) + (1 - c_{Cl^-}(t)/c_{Cl^-}(o))} \quad (3)$$

The value of $S_{Cl^-}^{SO_4^{2-}}$ is in the range of -1 to 1 . If the value was above 0 the current is primarily loaded by Cl^- , implying the migration is faster than SO_4^{2-} , and vice versa.

2.4. Analytical methods

The concentration of chloride in acid and salt compartments was determined by precipitation titration method using silver nitrate solution. Sulfate was measured using ion chromatography (IC) (DIONEX, ICS-2100). The corresponding acidity and basicity produced by BPM were obtained through acid-base titration with phenolphthalein and methyl orange as indicator. The variation of pH and conductivity of FGD brine in salt compartment were continuously monitored by pH meter (Thermo Orion, 230A+) and conductivity meter (LEICI, PXSJ-216F), respectively. And the voltage across the stack was directly recorded displayed on the screen supplied by the regulated CV/CC power supply.

3. RESULTS AND DISCUSSION

3.1. Acid and base generation

Fig 2 shows the concentration variations of acid and base as the time elapses. It can be found on increasing the operation time, both acid and base concentration are increased due to the continuous water splitting on the intermediate catalyst layer of BPM.

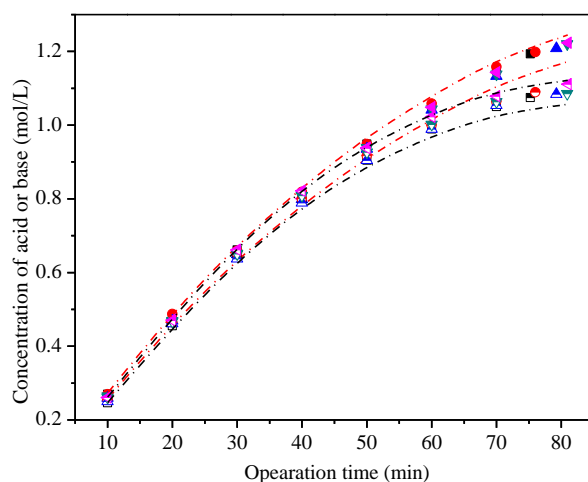


Figure 2. The concentration variation of acid (solid) and base (half up) as a function of operation time.

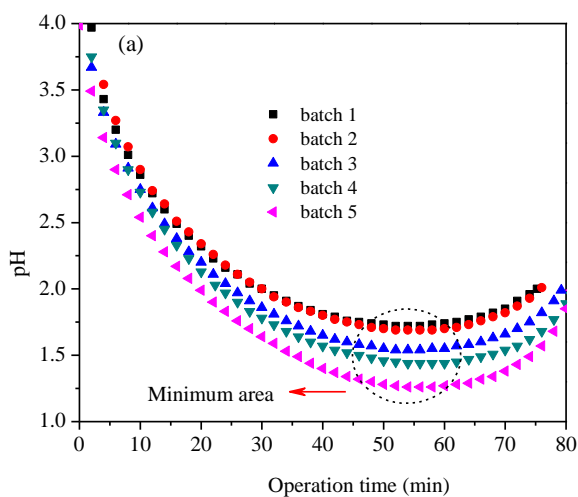
The five batches results indicate there is an insignificant difference in acid or base concentration with the statistical error below 3%. However, it can be seen the acidity is obviously higher than that of base compartment at the time above 60 min, which presents the different trend reported by previous works that acid concentration is lower due to the easy leakage of free H^+ in comparison to OH^- from acid compartment to salt compartment [16]. This phenomenon could be highly ascribed to the serious leakage of free H^+ in acid compartment resulting in the competition of free H^+ and Na^+ in salt compartment across the cation exchange membrane (discussed in Section 3.2) and the electroosmosis of water (discussed in Section 3.3). The final practical acidity and basicity

yielded are much less than the theoretical value of 1.53 mol/L and commercial product, but are suitable for resin regeneration [23], Ca and Mg removal and the pH adjustment instead of commercial purpose. This reuse process can decrease the expense of acid-base outsourcing so as to create extra economic benefit to offset the high cost of BMP.

3.2. Co-ions leakage of free H^+ and OH^-

Co-ions leakage of free H^+ and OH^- from AEM and CEM has historically been the problem for getting high concentrated acid and base products since the intrinsic mobility of both ions are considerably high. The transport number of both ions through ion exchange membrane increase with the produced acid and base concentration which also lead to their low concentration in the acid and base compartment [24], in particular for proton, the transport process could be easily implemented among water molecules due to the so-called “tunnel transport mechanism” [14]. Fig 3 displays the evolution of pH in the salt compartment with the different five batches. As seen from Fig 3, on increasing the salt concentration (in the order of batch 1 to batch 5), the pH becomes more acidic. This can be explained by the small initial salt volume to maintain the salt content giving rise to the high proton concentration. Additionally, all the five experimental tests show the increasing trend on the pH when the operation time above the region of 50-60 min. This phenomenon can be explained by the H^+ transfer from salt compartment to base compartment. At the early stage of BMED running, the H^+ concentration in the salt compartment from acid leakage is low in contrasted to Na^+ , the current is mainly loaded by Na^+ , which induces to the accumulation of H^+ resulting in the decline of pH. With the continuous decrease of Na^+ due to desalination, the H^+ concentration becomes comparable to Na^+ and gradually dominates the transport process leading to the increase of pH.

In addition, the difference between free H^+ in the acid compartment and OH^- in the base compartment is further discussed. It should be noted the total acidity measured mainly consists of free H^+ and the proton from HSO_4^- , nevertheless, the HSO_4^- would not participate in the leakage process. Fig 3(b) shows the fraction of SO_4^{2-} and HSO_4^- as a function of different total sulfate (S_T) in the acid compartment with the varied pH ranges.



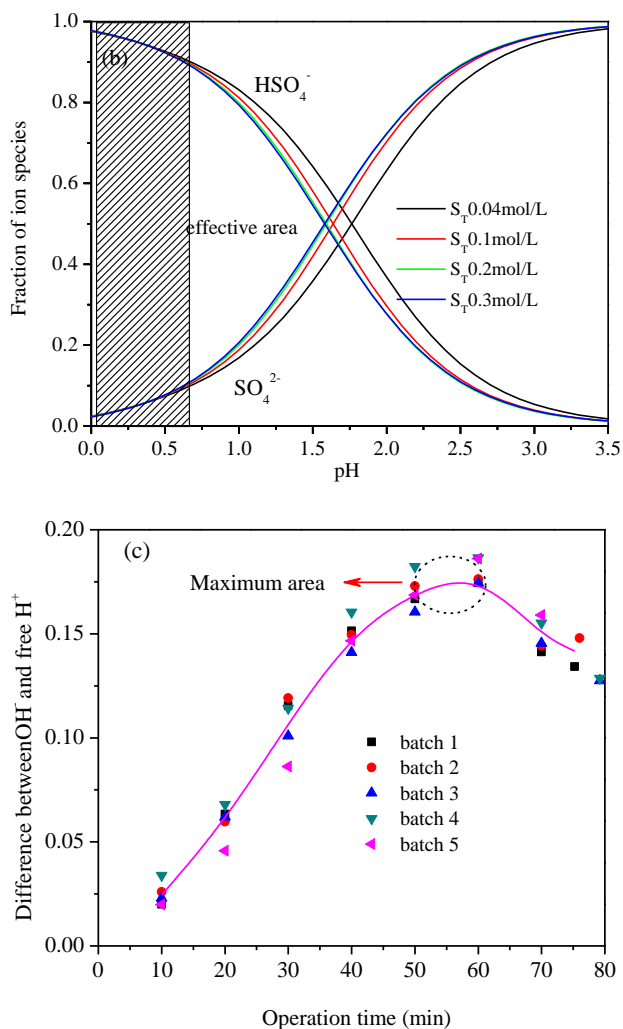


Figure 3. (a) The evolution of pH in the salt compartment at different operation conditions. (b) The distribution of SO₄²⁻ and HSO₄⁻ in the acid compartment with the pH varied. (c) The trend of concentration difference between OH⁻ and free H⁺ during BMED process.

The effective area means the running time of BMED setup in the range of 10 to 80 min. It could be found the proportion of HSO₄⁻ in this area is in excess of 90% of the total S_T in the acid solution. Hence, free H⁺ participated in leakage in the acid compartment can be approximatively expressed as the difference value between total acidity and S_T.

It can be seen in Fig 3(c) the concentration gap between OH⁻ and free H⁺ during the all BMED processes presents the parabola shape, where the maximum area is occurred at 50-60 min as well, highly confirmed to the minimum area appeared at 50-60 min in Fig 3(a), suggesting the H⁺ transport from salt to base compartment

3.3 Electroosmosis and forward osmosis

Water transport between salt and acid/base compartment is another important factor that limit the increase of acid and base concentration. Water molecules in the solution can be migration together

with SO_4^{2-} , Cl^- and Na^+ ions as the hydrated ion form, this phenomenon can be called “electroosmosis effect” [25]. On the other hand, the forward osmosis effect driven by the osmotic pressure resulted from concentration gradient between acid/base and salt solution is also related to the volume change. Fig 4 displays the volume change of acid, base and salt compartment during BMED operation. The volumes in either acid or base compartment are linearly increased [26] with the volume incremental quantity of base significantly greater than that of acid. The higher volume in base compartment may be responsible for the lower base concentration illustrated in Fig 2. However, in the terms of acid compartment, all the five batches tests show almost no obvious alteration of solution volume, in contrast to base solution that the volume is decreased with the enhancement of initial salt concentration due to strong forward osmosis effect (*i.e.* the shift of water molecules from base solution to salt solution). It could be inferred that the water transport from salt to acid compartment through CEM is entirely resulted from electroosmosis effect. In addition, it should be pointed out compared to the influence of forward osmosis for base volume, electroosmosis is regarded as the governing factor [27]. Therefore, some measures should be taken to diminish or eliminate this effect. According to the previous work reported by Jiang et al [28], this purpose can be efficiently realized by decreasing the hydrophilic nature of ion exchange membrane or breaking the hydrate ion form.

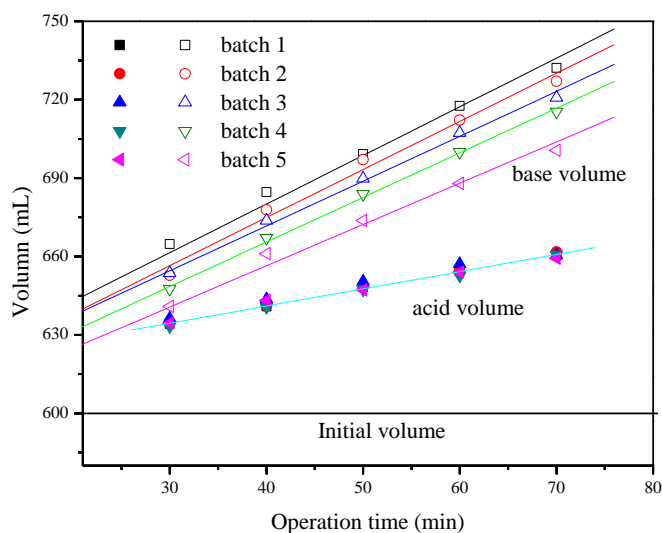
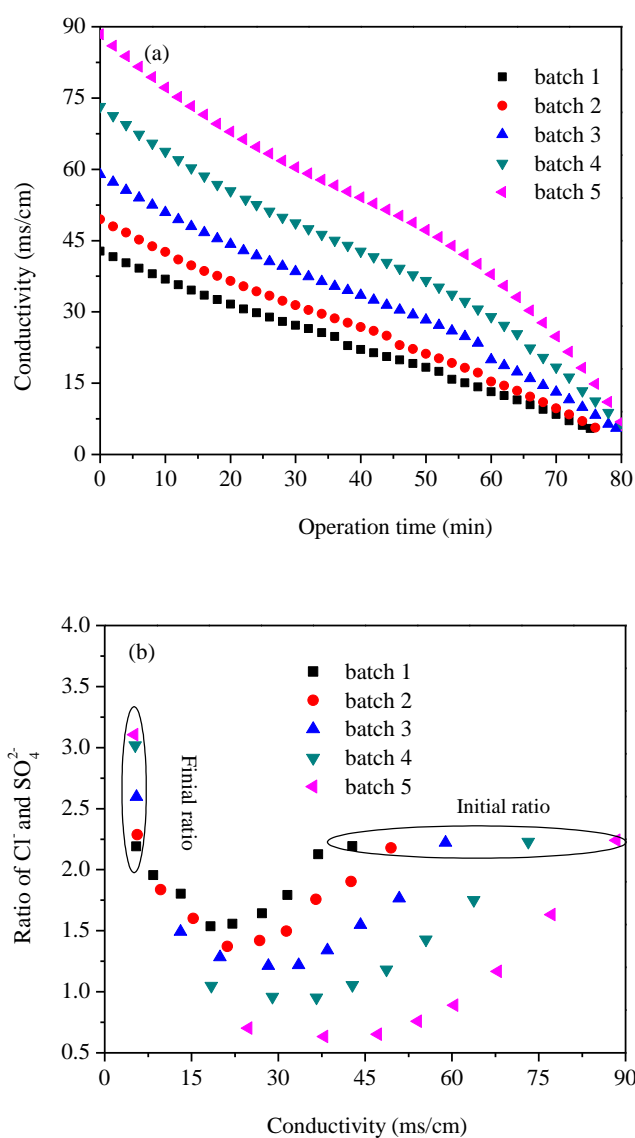


Figure 4. Volume change of acid, base and salt compartment during BMED operation

3.4. Migration of SO_4^{2-} and Cl^-

Similar to traditional electrodialysis process, the salt solution in BMED is steadily desalted with transfer of salt ions to acid/base compartment (*i.e.* Na^+ to base compartment and $\text{Cl}^-/\text{SO}_4^{2-}$ to acid compartment in this work) accompanied by the conductivity declined almost in a linear form (shown in Fig 5(a)). Considering the ternary mixture of anions in the FGD brine, the transport process of SO_4^{2-} and Cl^- is further discussed at the different salt concentrations. Fig 5(b) showed the molar ratio of remaining $\text{Cl}^-/\text{SO}_4^{2-}$ in the salt solution. As suggested from Fig 5(b), the molar ratio of $\text{Cl}^-/\text{SO}_4^{2-}$ is lowered in the first part of desalination. At a certain point in the desalination extent, the Cl^- removal

rate starts to decrease and a relative bigger part of the current is loaded by SO_4^{2-} , resulting in an increase in the remaining $\text{Cl}^-/\text{SO}_4^{2-}$ ratio in the salt solution and such variations are reinforced at higher initial salt concentration. With respect to the lower $\text{Cl}^-/\text{SO}_4^{2-}$ ratio in earlier stage for acid production, it should be attributed to the higher diffusion coefficients of Cl^- in comparison with SO_4^{2-} and the higher concentration of Cl^- in the initial solution, therefore, concentration polarization becomes less pronounced for Cl^- [29]. In order to effectively evaluate the separation efficiency between Cl^- and SO_4^{2-} , the selectivity coefficient is applied (Fig 5(c)). In batch 5, the selectivity coefficient $S_{\text{Cl}^-}^{\text{SO}_4^{2-}}$ is up to 0.6 at first 30 min far away from the batch 1. As the BMED operation proceeded, the selectivity coefficient gradually decreases. It can be inferred the HCl in the acid compartment can be first produced when the initial salt concentration is enhanced, suggesting the high purity HCl with little H_2SO_4 contamination in the earlier acid production.



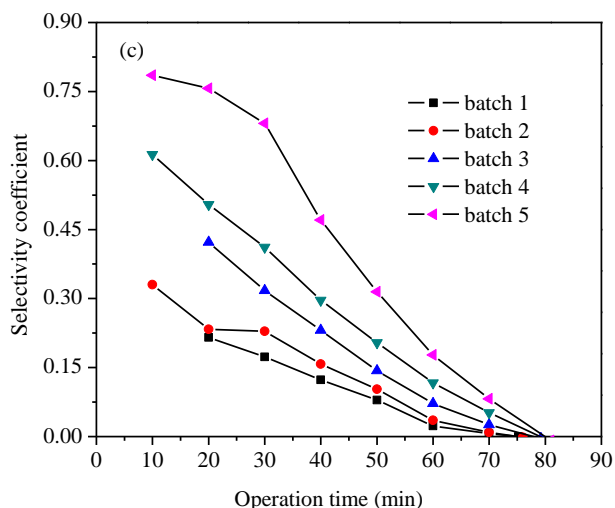


Figure 5. (a) The variation of conductivity, (b) molar ratio of remaining $\text{Cl}^-/\text{SO}_4^{2-}$ and (c) separation efficiency of Cl^- and SO_4^{2-} in the salt compartment at different operation time.

3.5. Current efficiency and energy consumption

Current efficiency and energy consumption are the two important parameters which determine the feasibility of any electrochemical process for higher process efficiency. Any system having higher current efficiency with lower energy consumption is considered to be the most favorable [30]. The current efficiency of OH^- and energy consumption of NaOH production at the five batch experiments are shown in Fig 6. It is observed the all current efficiency of BMED stack decreases near-unanimously along with the increase of operation time without significant difference (the difference of the five batches at time 10 min is caused by measuring error of volume). Once the operation time surpass the critical threshold (*i.e.* 40 min), the current efficiency drops sharply. This can be explained by the accentuated OH^- leakage and the migration of H^+ from salt compartment neutralizing base product.

In the case of energy consumption, low initial salt concentration such as batch 1 shows the higher energy consumption than the other batches. The increase in the energy consumption was mainly used to overcome the electrical resistance to generate joule heat [31]. When the salt concentration is increased to $\times 2$ of original compositions (batch 4), the energy consumption for generating 1.05 mol/L base is 2.14 Kwh/kg, significantly lower than the 2.34 Kwh/kg from the original FGD brine (batch 1) and 2.66 Kwh/kg reported by Reig et al [15] in the treatment of seawater desalination brines. Further enhancing the salt concentration shows only 0.07 Kwh/kg reduction (batch 5). In a word, appropriate concentration for $\times 2$ of FGD brine is beneficial for acid/base production. Just like current efficiency, the critical threshold at 40 min has also been found in Fig 6(b). The higher energy consumption in the subsequent acid/base production can be mainly owed to the co-ion leakage since the influence of solution electrical resistance can be neglected due to the high conductivity (Fig 5(a)). Therefore, developing a new ion exchange membrane that can effectively impede H^+/OH^- leakage is the key point to further decrease the energy consumption.

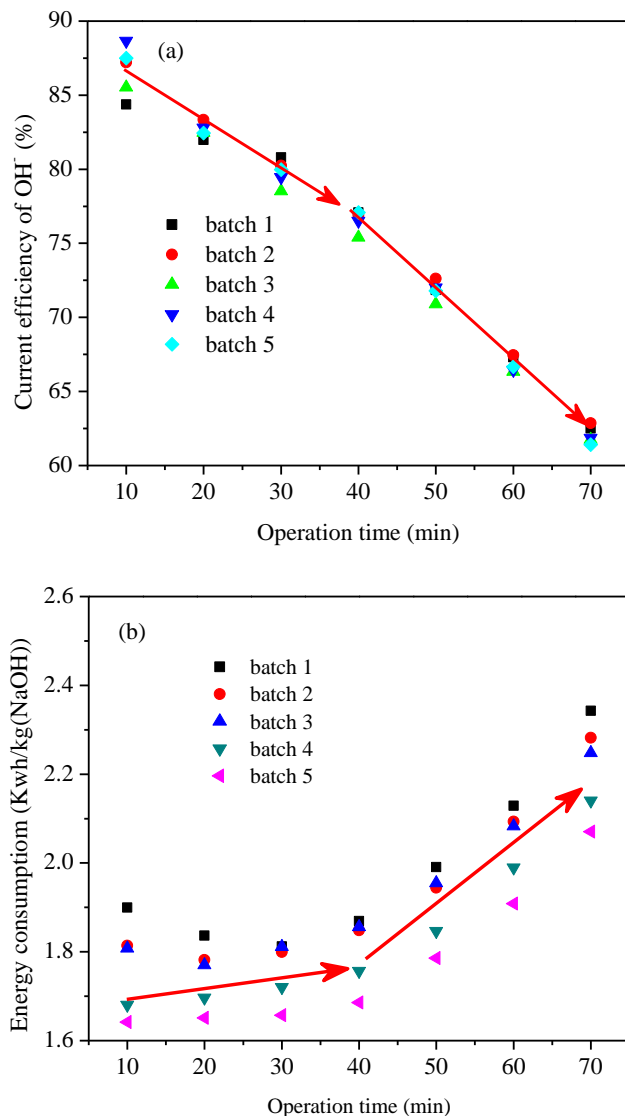


Figure 6. (a) Time dependency of (a) current efficiency and (b) energy consumption at different operation conditions (arrows represent the trend)

4. CONCLUSION

The flue gas desulfurization (FGD) brine in the thermal power plant has a high salinity mainly composed of NaCl and Na₂SO₄ after softening operation. In order to response environmental policy of zero discharge and take full advantage of this waste salt, a novel-innovative bipolar membrane electro dialysis (BMED) technique is selected and the application feasibility of simulated FGD brine treated by a lab-scale BMED system in terms of technical and economical parameters was evaluated in the work. The results indicate the BMED can be considered a technically feasible option for producing greater than 1 mol/L acid/base that can be potentially used for resin regeneration. Under the fixed salt content, initial FGD concentration shows different influence for the parameters such as acid/base production, co-ion leakage, water transfer, ion migration, current efficiency and energy consumption.

Suitable concentration for $\times 2$ of FGD brine can be responsible for the decrease of production cost from 2.34 to 2.14 Kwh/kgNaOH. And the energy consumption in the later acid/base production is strongly resulted from co-ion leakage. The results of this study have crucial implications in the case of resource utilization of FGD brine. Further study regarding real FGD brine is desired to prove in the next work.

ACKNOWLEDGEMENTS

The authors are thankful for the support of Wuhan University, China for supply of equipment and chemicals needed to complete this work. This research has been supported by National Natural Science Foundation of China (51602228).

Reference

1. K. Ghyselbrecht, A. Silva, B. Van Der Bruggen, K. Boussu, B. Meesschaert, L. Pinoy, *J. Environ. Manage.*, 140 (2014) 69.
2. S.C. Ma, J. Chai, G. D. Chen, W. J. Yu, *Renew. Sust. Energ. Rev.*, 58 (2016) 1143.
3. S. Casas, C. Aladjem, J. L. Cortina, E. Larrotcha, L. V. Cremades, *Solvent Extra. Ion Exc.*, 30 (2012) 322.
4. V. G. Gude, *Renew. Sust. Energ. Rev.*, 45 (2015) 52.
5. G. D. Enoch, W. F. Van Den Broeke, W. Spiering, *J. Membrane. Sci.*, 87 (1994) 191.
6. Y. H. Huang, P. K. Peddi, C. Tang, H. Zeng, X. Teng, *Sep. Purif. Technol.*, 118 (2013) 690.
7. R. L. Mcginnis, N. T. Hancock, M. S. Nowosielski-slepown, G. D. Murgan, *Desalination*, 312 (2013) 67.
8. J. Morillo, J. Usero, D. Rosado, H. E. Bakouri, A. Riaza, F. Bemaola, *Desalination*, 336 (2014) 32.
9. J. R. Davis, Y. Chen, J. C. Baygents, J. Farrell, *Acs Sustain. Chem. Eng.*, 3 (2015) 2337.
10. C. Fernandez-gonzalez, A. Dominguez-ramos, R. Ibanez, Y. Chen, A. Irabien, *Desalination*, 406 (2017) 16.
11. M. Reig, S. Casas, C. Valderrama, O. Gibert, J. L. Cortina, *Desalination*, 398 (2016) 87.
12. K. Ghyselbrecht, M. Huygebaert, B. Van Der Bruggen, R. Ballet, B. Meesschaert, L. Pinoy, *Desalination*, 318 (2013) 9.
13. M. Badruzzaman, J. Oppenheimer, S. Adham, M. Kumar, *J. Membrane Sci.*, 326 (2009) 392.
14. R. Ibanez, A. Perez-gonzalez, P. Gomez, A. M. Urriaga, I. Ortiz, *Desalination*, 309 (2013) 165.
15. M. Reig, S. Casas, O. Gibert, C. Valderrama, J. L. Cortina, *Desalination*, 382 (2016) 13.
16. J. Shen, J. Huang, L. Liu, W. Ye, J. Lin, B. Van Der Bruggen, *J. Hazard. Mater.*, 260 (2013) 660.
17. Y. Wei, C. Li, Y. Wang, X. Zhang, Q. Li, T. Xu, *Sep. Purif. Technol.*, 86 (2012) 49.
18. J. LIN, W. YE, J. HUANG, B. Ricard, B. Van Der Bruggen, *Acs Sustain. Chem. Eng.*, 3 (2015) 1993.
19. A. T. K. Tran, P. Mondal, J. Y. Lin, B. Meesschaert, L. Pinoy, B. Van Der Bruggen, *J. Membrane. Sci.*, 473 (2015) 118.
20. S. Casas, C. Aladjem, E. Larrotcha, G. Oriol, C. Valderrama, J. L. Cortina, *J. Chem. Technol. Biot.*, 89 (2014) 872.
21. C. Li, G. Wang, H. Feng, T. He, Y. Wang, T. Xu, *Sep. Purif. Technol.*, 156 (2015) 391.
22. B. Van Der Bruggen, A. Koninckx, C. Vandecasteele, *Water Res.*, 38 (2004) 1347.
23. V. Mavrov, H. Chmiel, B. Heitele, F. Rogener, *Desalination*, 124 (1999) 205.
24. X. Wang, Y. Wang, X. Zhang, T. Xu, *Bioresource technol.*, 125 (2012) 165.
25. J. S. Jaime-ferrer, E. Couallier, P. Viers, G. Durand, M. Rakib, *J. Membrane Sci.*, 325 (2008) 528.
26. M. Mier, R. Ibaez, I. Ortiz, *Sep. Purif. Technol.*, 59 (2008) 197.
27. C. Jiang, Y. Wang, Z. Zhang, T. Xu, *J. Membrane. Sci.*, 450 (2014) 323.
28. C. Jiang, Q. Wang, Y. Li, T. Xu, *Desalination*, 365 (2015) 204.

29. A. Galama, G. Daubaras, O. Burheim, H. H. M. Rijnaarts, J. W. Post, *J. Membrane Sci.*, 452 (2014) 219.
30. L. Bazinet, D. Ippersiel, C. Gendron, J. Beaudry, B. Mahdavi, J. Amiot, F. Lamarche, *J. Membrane Sci.*, 173 (2000) 201.
31. K. Venugopal, S. Dharmalingam. *Desalination*, 344 (2014) 189.

© 2018 The Authors. Published by ESG (www.electrochemsci.org). This article is an open access article distributed under the terms and conditions of the Creative Commons Attribution license (<http://creativecommons.org/licenses/by/4.0/>).